PROGRESS IN COATING THEORY

by

Norbert ALLEBORN

Review paper
UDC: 621.793:666.1.055:678.026
BIBLID: 0354-9836, 5 (2001), 1, 131-152

This paper is dedicated to the 60th birthday of Prof. Dr. Dr. h.c. Franz Durst, head of the Institute of Fluid Mechanics in Erlangen (LSTM-Erlangen). It summarizes work performed at LSTM-Erlangen on liquid film coating and drying, with emphasis on recent developments, particularly in curtain coating and direct condensation drying. Liquid film coating of continuous webs comprises various tasks, ranging from fluid distribution in a coating die over reliable operation of the application process to defect-free and economical drying. These tasks are subject of research efforts at LSTM-Erlangen to acquire a fundamental understanding of the physical mechanisms involved in coating and drying and to develop from it process engineering working tools for design and operation of coating equipment.

INTRODUCTION

Coating with thin liquid layers is an important process step in manufacturing of numerous high quality products. Photographic films, magnetic tapes or teststripes for chemical or medical analysis carry one or multiple layers on a substrate which provide the function of the product. Coating of metal sheets, polymer foils and paper, in addition, protects the substrate and improves its optical appearance. Paper used for printing applications is coated with a pigment layer to achieve a smoother surface and a defined porosity in order to avoid excessive sorption and spreading of the printing colors. Besides improving the functionality, the pigment layer also provides an improved stiffness and better optical properties of the paper.

In liquid film coating, the coating substance is suspended or dissolved in a solvent, such as water or (mixtures of) organic fluids, in order to facilitate transport and deposition on the substrate. The coating process itself, illustrated in Fig. 1 for curtain coating of continuous substrates, consists essentially of three major parts:

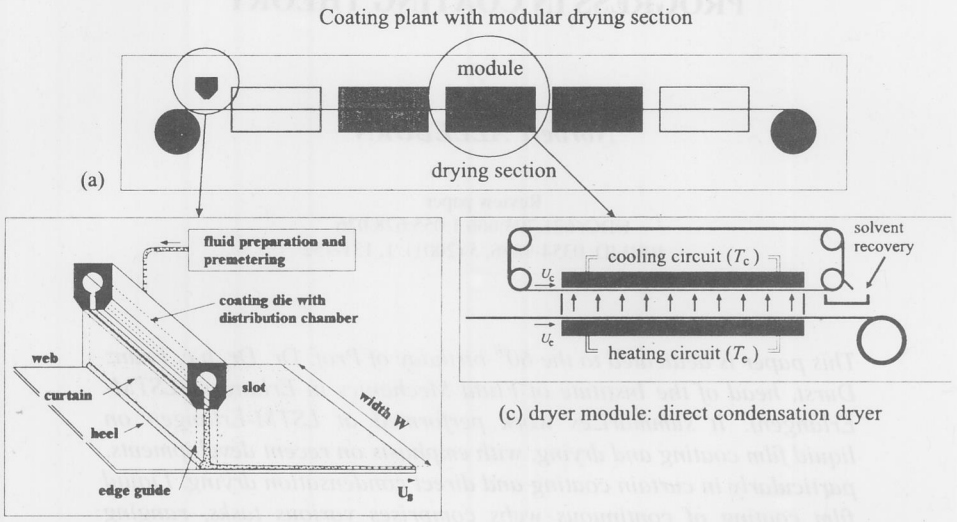

Figure 1. Sketch of a coating plant for paper coating

(a) Fluid distribution

The coating layer has to be deposited onto a moving continuous substrate (web) which can be up to 10 m wide, as *e. g.* in paper production. An even distribution of the coating fluid across the substrate width is an important prerequisite for the subsequent coating steps. Especially for premetered coating methods, to be described later, a high uniformity of the fluid distribution is essential. Thickness variations of the light sensitive layers of a photographic film in the range of about 1 μm, for instance, can already be detrimental to the product quality. The design of the geometry of the internal coating die cavities has to take into account a complicated interplay of viscous and inertial forces governing the fluid flow in dependence on rheology and operation parameters [22]. Therefore, a mathematical model for the design of coating die cavities has to capture the essential physical mechanisms determining the flow while being sufficiently simple to allow an efficient implementation as working tool for finding an optimum geometry that gives uniform distribution in the desired range of operation, taking into account mechanical aspects such as the influence of manufacturing inaccuracies on flow distribution. A software package for die design developed at LSTM-Erlangen [17] exploits the mathematical concept of inverse problems as a powerful tool for computing an optimum geometry under constraints such as a lower limit for wall shear stresses or an upper limit for residence time of the fluid in the die.

(b) Application of the coating fluid

Subsequent to fluid distribution the coating fluid has to be transferred to the moving continuous web. In *self-metered coating methods* (cf. [19], chapter 12), such as for instance blade coating [12, 13, 23] and roll coating [14], the coating liquid is in a first step applied in excess either to the web directly or onto an applicator roll from which it is eventually transferred to the web. In a second step a metering element is used to remove the excess amount of fluid leaving a uniform thin film of the required thickness. A detailed knowledge of the flow in the metering element is therefore necessary for predicting the metered film thickness. *Premetered coating methods* (cf. [10], and also chapter 11 of [19]), such as slot coating [20, 27] or curtain coating [20, 25] apply precisely the required amount of coating fluid in a single step. The flow rate $q = U_s W h$ which is determined by the web speed, U_s, the machine width, W, and the desired liquid film thickness on the paper, h, is controlled by a flow meter. Due to its high accuracy particularly in the range of flow rates typical for coating, the Coriolis flow meter appears to be a suitable choice for this task [17, 21].

Important from a process engineering viewpoint is a detailed picture of the range of fluid properties and operation parameters in which a certain coating method allows a precise application of the coating fluid and a reliable operation of the whole process. The limits of operation mark out the coating window of the process in the parameter space. The location of those limits depends strongly on the sensitivity of the coating flow towards external perturbations such as flow rate fluctuations or mechanical vibrations. If perturbations grow with time the flow is unstable and can not be used for coating. Even if small perturbations decay with time in a stable flow, however, they can still leave traces on the coated film and impair its function. A major aim in coating research is therefore the determination of the coating window and an investigation of stability and sensitivity of coating flows [3, 4, 20]. A strong thrust to explore the operation limits of a process and possibly shift them towards higher production speeds comes from the need for an economical mass production. In paper industry coating is already done at web speeds of 3000 m/min. Besides increasing speed, the development of improved coating processes that produce, for instance, the desired paper quality using less pigments while yielding a lower area weight of the paper, poses a future challenge to coating research, given a production of about 13 million tons of coated paper in Western Europe.

(c) Drying

Once the coating fluid has been deposited evenly on the web, the solvent has to be removed in order to immobilize the coating substance. In a thermal drying process heat is supplied to evaporate the solvent and the solvent vapor is removed by an inert carrier gas. When designing or operating a coating plant, the drying section requires special attention: Excessive heat transfer into the film may cause numerous coating defects, *e. g.* crater formation due to boiling of the solvent, that ruin all efforts for a smooth and even application of the layer in the preceding coating steps. Overheating may trigger unwanted chemical reactions that damage the functionality of the final product or may even pose a

health hazard, as *e. g.* in food packaging. Coating defects and handling requirements of solvent and coating substance, as for instance boiling or explosion limits, impose constraints on the drying operation which, in consequence, limit the achievable production speed. The required energy for the drying process makes up a considerable part of the total production costs, so that the drying section is a major factor for the efficiency and profitability of the entire coating process [8]. A working tool for predicting the solvent transport in the liquid film and to evaluate the dryer performance, including aspects of energy consumption and exhaust air treatment, is therefore an important prerequisite for both appropriate design and successful operation of a drying section. For air impingement and floatation dryers, being widely used in industry, a numerical model has been developed at LSTM-Erlangen for computing solvent content and temperature in the film along a modular drying section and for optimizing energy consumption [6, 7]. Besides optimizing conventional drying methods, there is also a strong need to explore new drying methods that reduce energy consumption and pollution arising from organic solvents in the exhaust air of the dryer. A reduction by only a few percent of the energy required for drying of the paper produced in Western Europe, for instance, could imply already savings in the order of a few millions Euro. In addition, the aspect of solvent recovery gains importance in the light of a consumption of 81,000 tons of organic solvents per year in coating and printing industry. For this reason, the concept of direct condensation drying which offers a potential for heat and solvent recovery has been investigated as an alternative to conventional drying methods [1].

In the following sections, research work performed at the LSTM-Erlangen in the field of coating and drying will be highlighted. Main emphasis will be put on recent work in curtain coating and film drying.

FLUID DISTRIBUTION: DESIGN OF DISTRIBUTION CHAMBERS IN COATING DIES

In premetered methods like slot coating or curtain coating the fluid is distributed across the machine width in a die. Aim of the design of the cavities inside the coating die is a uniform distribution of the fluid flow at the die exit, cf. Fig. 1(b). Basically, this could be achieved by a large cross section of the distribution chamber and a high pressure drop across the feed slot. However, this infinite cavity concept is limited by *constraints* such as a lower limit for the wall shear stress, to avoid settling and solidification of the fluid in the die, an upper limit for the residence time, to avoid ageing of the fluid and an upper limit for the pressure in the slot, to avoid mechanical deformation of the die. Relying on the mathematical concept of inverse problems, an optimized geometry of the cavity can be obtained for given fluid properties and operation parameters, taking into account operation constraints. Die optimization by solving inverse problems has been implemented at LSTM-Erlangen for one-dimensional equations for the fluid flow in the coating die [17]. Figure 2 shows, for illustration, flow profiles (flow rate per unit length) at the slot exit and the pressure in the first chamber for a coating die with two distribution chambers. For low Reynolds numbers Re viscous forces are dominant and the pressure drops from the inlet to the end of the first chamber, so that the mass flux out of the slot exit drops along the die.

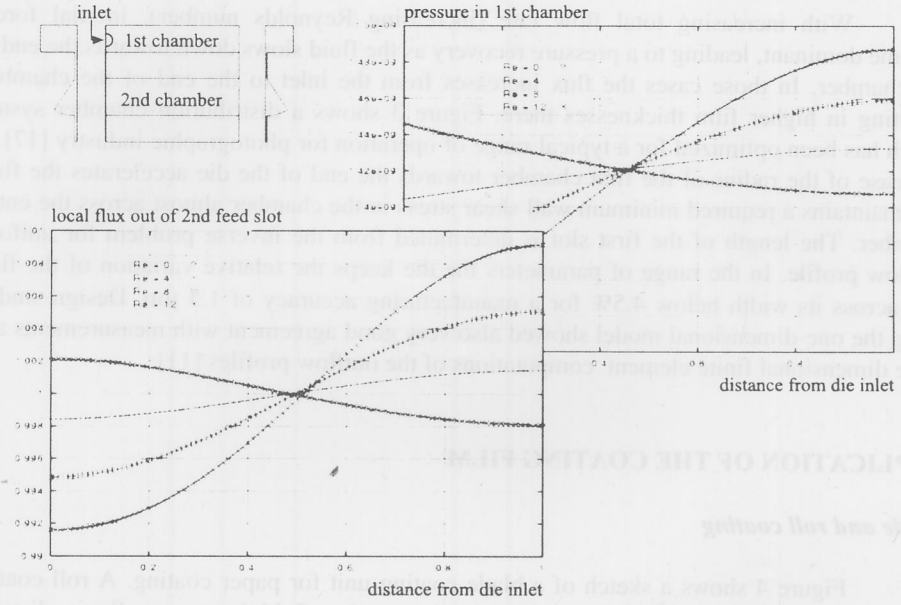

Figure 2. Fluid distribution in a coating die, $\mathrm{Re} = \rho\, \dot{q}_{gl} \,/\, \eta(\dot{\gamma}_{inlet})$

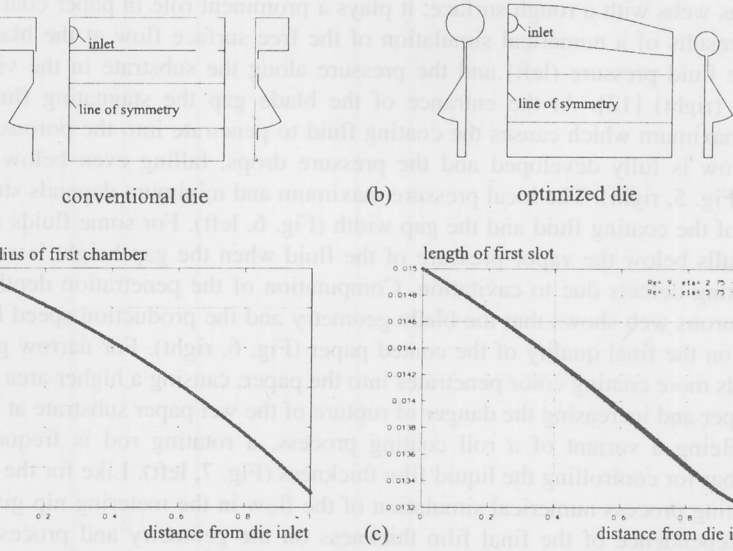

Figure 3. Optimization of a coating die

With increasing total flow rate (increasing Reynolds number), inertial forces become dominant, leading to a pressure recovery as the fluid slows down towards the end of the chamber. In those cases the flux increases from the inlet to the end of the chamber, resulting in higher film thicknesses there. Figure 3 shows a distribution chamber system which has been optimized for a typical range of operation for photographic industry [17]. A decrease of the radius of the first chamber towards the end of the die accelerates the fluid and maintains a required minimum wall shear stress in the chamber almost across the entire chamber. The length of the first slot is determined from the inverse problem for uniform outflow profile. In the range of parameters the die keeps the relative variation of the flow rate across its width below 4.5% for a manufacturing accuracy of 1.5 μm. Design studies using the one-dimensional model showed also very good agreement with measurements and three dimensional finite element computations of the outflow profiles [11].

APPLICATION OF THE COATING FILM

Blade and roll coating

Figure 4 shows a sketch of a blade coating unit for paper coating. A roll coating device (flooded nip) is used here to apply the coating fluid in excess. Some distance downstream of the flooded nip, a thin elastic blade is pressed against the coated paper substrate on the backing roll where it scratches off the excess amount of the coating fluid. The height H_R of the blade gap results from a balance between elastic and fluid forces and it determines the final wet film thickness on the web (Fig. 4, right). Blade coating is used to coat porous webs with a rough surface; it plays a prominent role in paper coating. Figure 5 shows as results of a numerical simulation of the free surface flow at the blade a contour plot of the fluid pressure (left) and the pressure along the substrate in the vicinity of the blade gap (right) [12]. At the entrance of the blade gap the stagnating fluid induces a pressure maximum which causes the coating fluid to penetrate into the porous web. In the gap the flow is fully developed and the pressure drops, falling even below atmospheric pressure (Fig. 5, right). The local pressure maximum and minimum depends strongly on the rheology of the coating fluid and the gap width (Fig. 6, left). For some fluids the minimum pressure falls below the vapor pressure of the fluid when the gap height is small and may cause coating defects due to cavitation. Computation of the penetration depth of the fluid into the porous web shows that the blade geometry and the production speed have a strong influence on the final quality of the coated paper (Fig. 6, right). For narrow gaps and high web speeds more coating color penetrates into the paper, causing a higher area weight of the coated paper and increasing the danger of rupture of the wet paper substrate at high speeds.

Being a variant of a roll coating process, a rotating rod is frequently used as metering bar for controlling the liquid film thickness (Fig. 7, left). Like for the self-metering blade coating process numerical simulation of the flow in the metering nip gives an insight into the dependence of the final film thickness on the geometry and process parameters, shown in Fig. 7 (right) for rigid rolls, thus providing process engineering guidelines for ope-

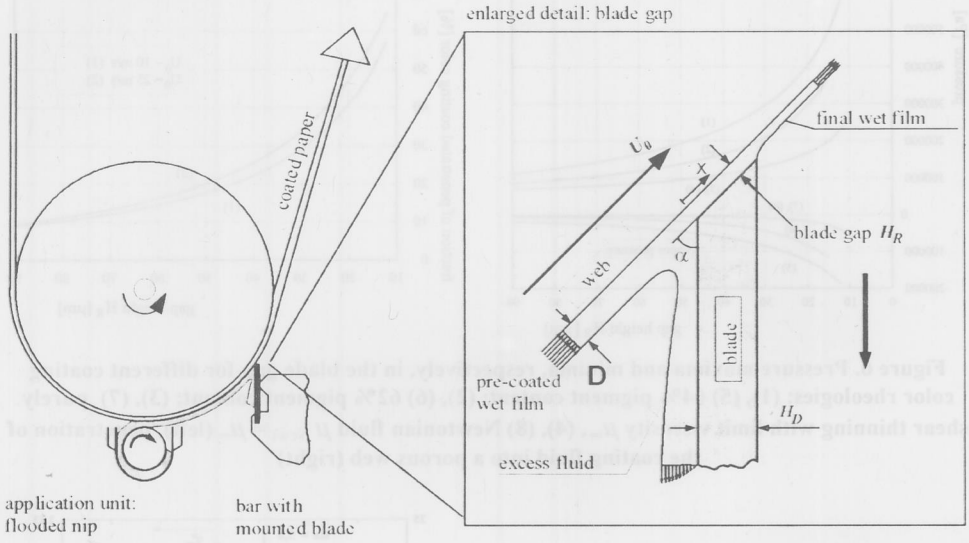

Figure 4. Sketch of blade coater for paper coating

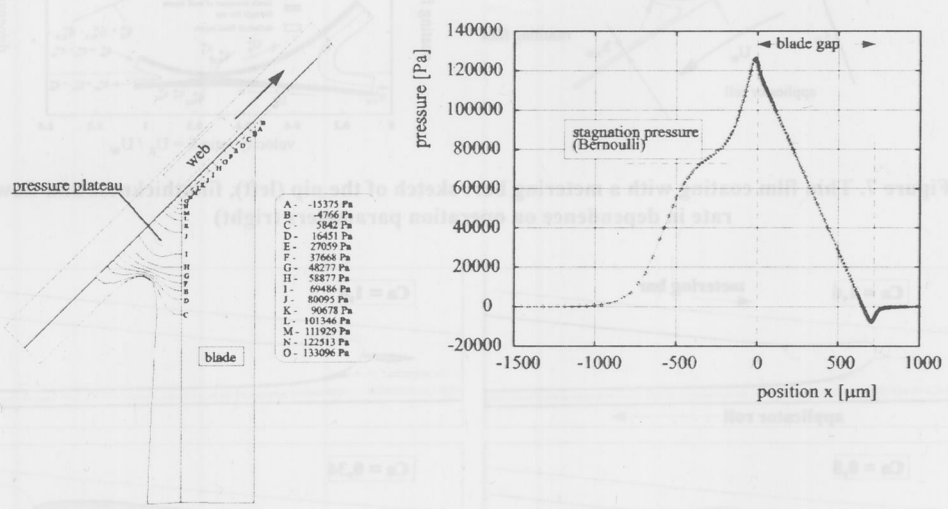

Figure 5. Pressure field and pressure along web in the blade gap

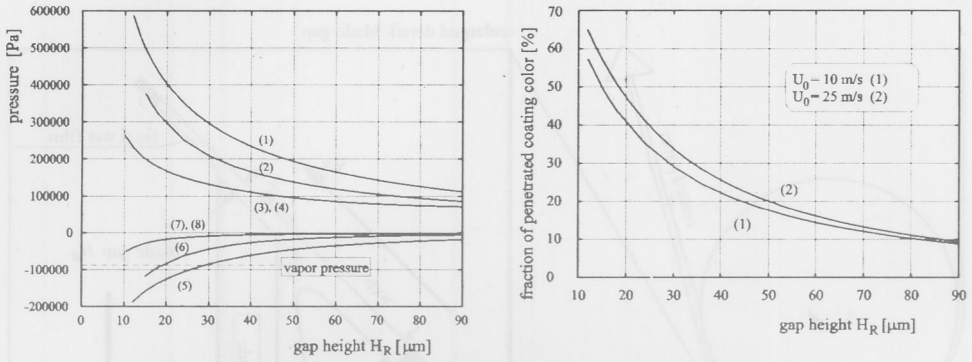

Figure 6. Pressure maxima and minima, respectively, in the blade gap for different coating color rheologies: (1), (5) 64% pigment content; (2), (6) 62% pigment content; (3), (7) purely shear thinning with limit viscosity μ_∞, (4), (8) Newtonian fluid $\mu_{Newt} = \mu_\infty$ (left), penetration of the coating fluid into a porous web (right)

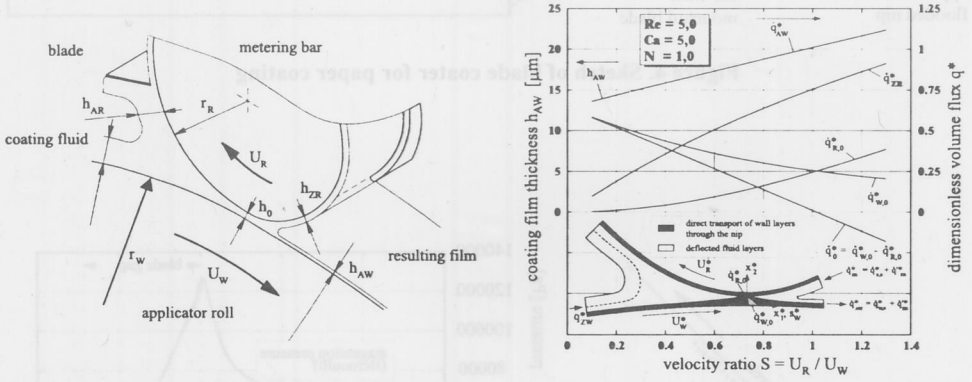

Figure 7. Thin film coating with a metering bar: sketch of the nip (left), filmthickness and flow rate in dependence on operation parameters (right)

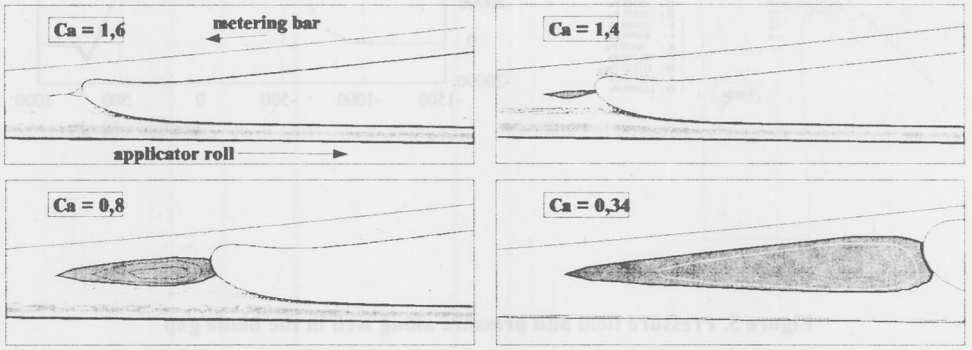

Figure 8. Thin film coating with a metering bar: streamlines at nip exit

ration (cf. Sünderhauf *et al.* in [9], pp. 379-384 and [14]). Details of the free surface flow in the nip which are resolved by the numerical simulation give additional information about possible implications on the process. Large recirculation eddies in the meniscus, as shown for capillary number Ca = 0.34 in Fig. 8, imply high residence times and therefore ageing of the fluid in the nip. Such eddies are unstable and tend to cause coating defects (ribbing instability).

Slot coating

In a slot coating process the distance between the coating die and the moving web is in the range of about 100 µm. The fluid exiting from the feed slot is dragged away be the web. The shape of the coating bead is determined by an interplay of flow rate, web speed, capillarity and external pressure difference between upstream and downstream meniscus (Fig. 9, left). A force balance taking into account the contributions of these effects determines the coating window of a slot coater [10, 20, 27]. Small perturbations, introduced for instance by external vibrations or oscillations of the flow rate, may cause thickness variations in cross web direction (barring, cf. Fig. 10). A linear stability analysis of the computed flow field reveals the sensitivity of a slot coater towards such perturbations [20]. The frequency spectrum of flow rate oscillations implies the existence of vibration modes that produce particularly strong film thickness variations on the coated web for low fluid viscosities (Fig. 9, right).

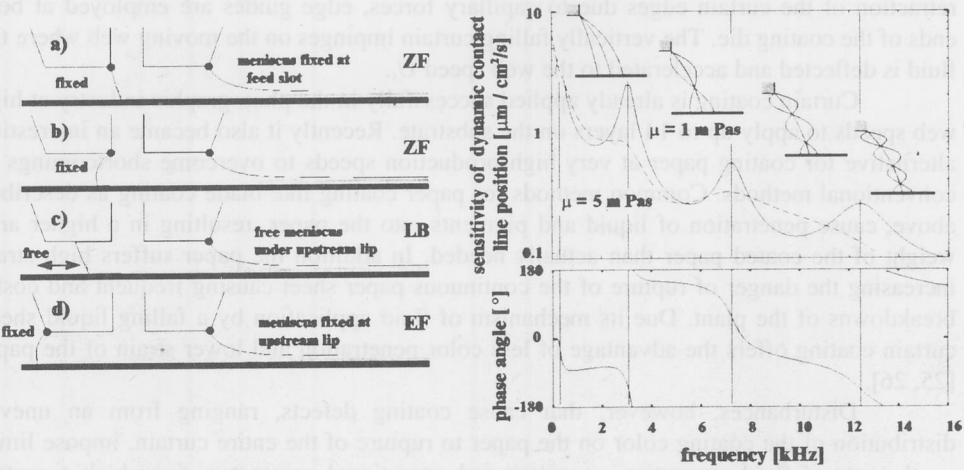

Figure 9. Slot coating: states of operation (left), sensitivity of contact line towards perturbations (right)

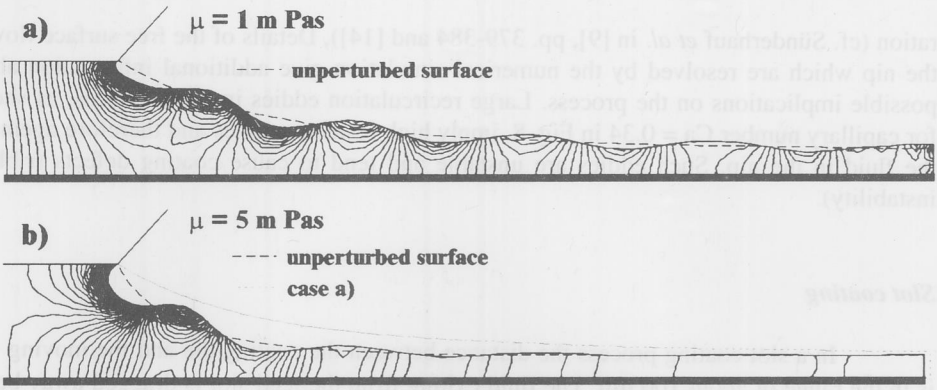

Figure 10. Slot coating: filmthickness perturbations (barring)

Curtain coating

In a curtain coating process the distance between the coating die and the moving web is in the order of about 100 mm. Figure 1(b) shows a sketch of a curtain coating device. A premetered volume flux per unit width $q = U_s h$, determined by the web speed, U_s, and the desired liquid film thickness on the substrate, h, is fed into the distribution chamber of the coating die where it gets evenly distributed across the machine width W. The coating die generates a freely falling thin liquid layer with two free surfaces, the curtain. To avoid retraction of the curtain edges due to capillary forces, edge guides are employed at both ends of the coating die. The vertically falling curtain impinges on the moving web where the fluid is deflected and accelerated to the web speed U_s.

Curtain coating is already applied successfully in the photographic industry at high web speeds to apply up to 14 layers on the substrate. Recently it also became an interesting alternative for coating paper at very high production speeds to overcome shortcomings of conventional methods. Common methods for paper coating like blade coating as described above, cause penetration of liquid and pigments into the paper, resulting in a higher area weight of the coated paper than actually needed. In addition the paper suffers high strain increasing the danger of rupture of the continuous paper sheet causing frequent and costly breakdowns of the plant. Due its mechanism of fluid application by a falling liquid sheet, curtain coating offers the advantage of less color penetration and lower strain of the paper [25, 26].

Disturbances, however, that cause coating defects, ranging from an uneven distribution of the coating color on the paper to rupture of the entire curtain, impose limits on the sets of fluid properties, geometry and operational parameters for which a curtain coating device can be used. Figure 11 illustrates qualitatively an operating window of a curtain coating process in the parameter space of flow rate, expressed dimensionless in terms of a Reynolds number $\mathrm{Re} = q/\nu$, and web speed, made dimensionless with the impingement velocity of the curtain.

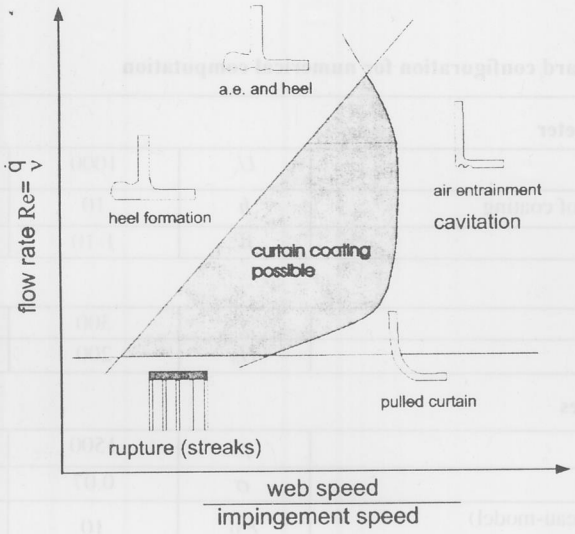

Figure 11. Operation window of curtain coating

The operation range of a curtain coating device is limited, on the one hand, by the rupture of the curtain followed by streak formation, if the flow rate is too small. If, on the other hand, the flow rate is too high, operation is limited by the formation of a heel, causing film thickness variation and air entrainment. While entrained air can be absorbed by the porous paper substrate in paper coating, the flow field in the impingement region can still affect the coating performance at high web speeds, where high shear rates can deflect the curtain (pulled curtain) and even cause cavitation.

A numerical computation of the free surface flow in the impingement zone of a liquid curtain falling onto a moving web, performed at LSTM-Erlangen, provides an insight into the physical mechanisms taking place especially at high web speeds [25]. Table 1 shows a standard configuration used for the numerical computations which is characteristic for curtain coating of paper. The rheology of coating colors used for paper coating can be suitably described by a Carreau model

$$\mu(\dot{\gamma}) = \mu_\infty + (\mu_0 - \mu_\infty)\left(1 + \frac{\dot{\gamma}^2}{\dot{\gamma}_c^2}\right)^{(n_c-1)/2}$$

which relates the dynamic viscosity μ with the shear rate $\dot{\gamma}$. The system of equations governing the free surface flow are solved numerically with the finite element code FIDAP [25].

Table 1. Standard configuration for numerical computation

Process parameter			
Web speed	U_s	1000	m/min
Film thickness of coating	h	10	μm
Paper width	W	1-10	m
Geometry			
Slot width	s	300	μm
Curtain height	H_0	200	mm
Fluid properties			
Density	ρ	1500	kg/m^3
Surface tension	σ	0.07	N/m
Viscosity (Carreau-model)	μ_0	10	Pa s
	μ_∞	0.04	Pa s
	$\dot{\gamma}_c$	1	1/s
	n_c	0.1	-

Fluid flow in the impingement region

Figure 12 shows the shape of the free surfaces of the impinging curtain as well as contours of speed and shear rate for a standard configuration described in Table 1. In the region of the falling curtain shown here, the two free surfaces remain almost parallel to each other and the influence of the moving web can not be felt at a distance of more than about 100 μm above the web. Below that distance the curtain contracts due to the acceleration of the fluid by the moving web. The contour lines of the fluid speed $|\vec{u}|$, plotted in Fig. 12(a) normalized to the impingement velocity V_A, show that fluid acceleration starts already some distance above the web. Close to the web, within about a distance of the final film thickness h, however, the major part of the fluid acceleration takes place. The falling curtain is sheared off and the fluid is accelerated to web speed in a Sakiadis boundary layer along the web, starting from the contact line of the rear curtain surface with the web. The boundary layer grows along the direction of the web motion and reaches the free film surface after a short distance of slightly more then 120 μm. This acceleration process implies high shear rates in the impingement region which vary over four orders of magnitude in that region, as shown in Fig. 12(b). It turns out that the shear thinning behaviour, characterized by μ_∞ essentially determines the flow in the impingement region [25]. Figure 13 allows a closer look on the effect of shear thinning on the shape of the curtain, for a web speed U_s = 1800 m/min and a film thickness h = 6.7 μm: For strong shear thinning, *i. e.* low values of μ_∞ (cf.

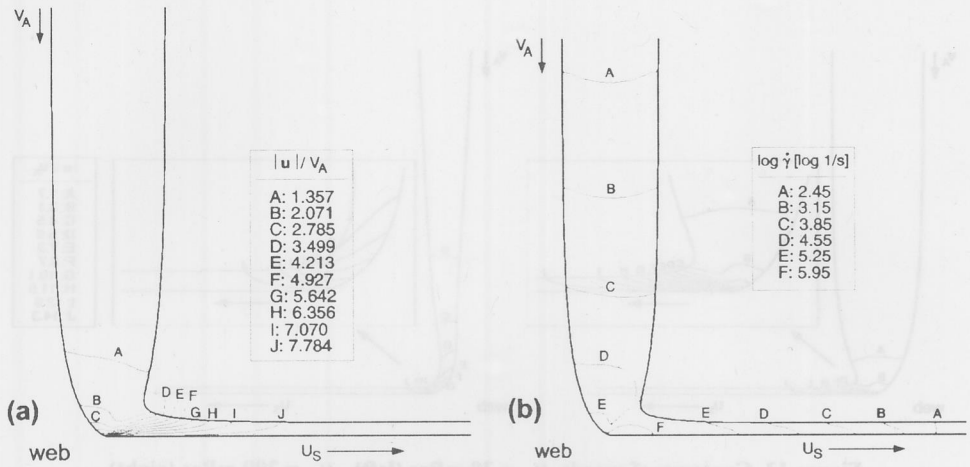

Figure 12. Contours of speed (a) and shear rate (b) (standard configuration, Table 1)

Fig. 13, left), the curtain starts to contract close to the web. However, for higher values of μ_∞, *i. e.* weaker shear thinning behaviour of the coating color, the contraction sets in already far above the web. It is interesting to note that even though the accelerating effect of the moving web reaches farther upstream of the curtain the more viscous the color gets, the contraction of the free surfaces takes place almost symmetrically there, without any significant deflection of the centerline of the curtain. Only very close to the web a pulling effect of the web can be observed for higher values of μ_∞, cf. Fig. 13 (right), where the centerline is deflected and the contact line is located downstream of the front surface of the curtain.

In the case of high shear thinning ($\mu_\infty = 0.02$ Pas, Fig. 13, left) the geometry of the curtain is quite similar to the standard configuration (cf. Fig. 12), although the web speed is almost doubled and the viscosity only half of the standard case, so that the Reynolds-number

$$\mathrm{Re} = \frac{\rho h U_s}{\mu_\infty}$$

is more than twice higher here. An explanation for this behaviour is suggested in [25]: For the range of fluid viscosities relevant in paper coating, surface tension has only minor influence on the shape of the impingement region. The location of the contact line is mainly controlled by the length of the Sakiadis boundary layer. Using the solution of the boundary layer equation an approximation of the distance x_f of the contact line from the front surface of the curtain has been given in [18] as

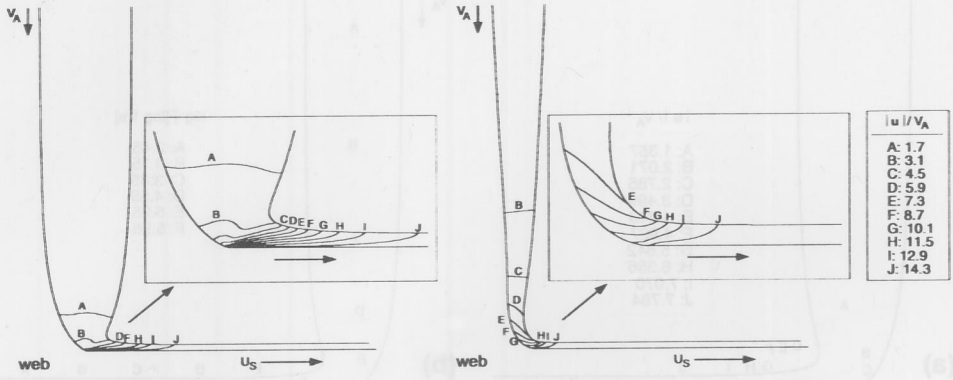

Figure 13. Contours of speed: $\mu_\infty = 20$ mPas (left), $\mu_\infty = 200$ mPas (right) ($U_S = 1800$ m/min, $h = 6.7$ μm)

$$\frac{x_f}{d_A} = \frac{V_A}{U_S}\,\mathrm{Re} = \frac{\rho h V_A}{\mu_\infty} = \Lambda\,.$$

The dimensionless quantity Λ can thus be considered as a measure for the geometry of the impingement region. For high values of Λ the impinging curtain is sheared off with a boundary layer developing along the moving web, as shown in Fig. 12(a) ($\Lambda = 0.77$) and Fig. 13 (left) ($\Lambda = 1.05$). For low values of Λ, *i. e.* for high viscosity μ_∞, the contact line moves to the right (in direction of web motion), towards the front free surface of the curtain. Fig. 13 (right) shows, that for $\mu_\infty = 0.2$ Pas ($\Lambda = 0.1$) the contact line is located even ahead of the front surface. Due to the high viscosity the acceleration of the fluid starts already far upstream in the curtain. Instead of being sheared off, the curtain is enlongated and deflected in the direction of the moving web. The velocity of the curtain has almost reached the web speed when it hits the moving web at the contact line, so that a pronounced boundary layer, as in the case of low values of μ_∞, is missing here. In the next section consequences of the strong deformation of the fluid in the impingement region will be discussed in more detail.

Cavitation in the impingement region

It is observed experimentally that high viscosity fluids can suffer cavitation when exposed to high shear rates. Archer *et al.* [5] and Streator *et al.* [24] found experimentally a critical shear rate for cavitation in the range of 0.1 to 0.3 MPa for fluid viscosities in the range of 0.02 Pas to 10^6 Pas. Joseph [16] derived a criterion of maximum stress which relates the elongational stress along the principal axes of the viscous part of the stress tensor to the onset of cavitation. It turns out that the commonly used criterion for cavitation, which

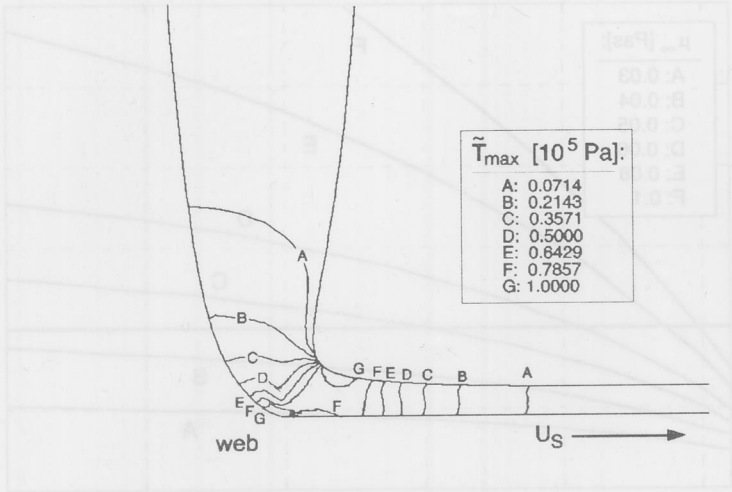

Figure 14. Contours of the critical stress (configuration of Table 1, μ_∞ = 0.08 Pas)

asserts onset of cavitation if the isotropic component of the stress tensor, $p = -1/3$ tr $\mathbf{T}$, falls below the (thermodynamic) vapor pressure p_c, is not a suitable cavitation criterion in pure shear flows. To apply the cavitation criterion given in [16], the viscous part $\mathbf{S}$ of the stress tensor

$$\mathbf{T} = -p\mathbf{I} + \mathbf{S}$$

is diagonalized so that the elongational viscous stresses of

$$\mathbf{S} = \begin{pmatrix} S_{11} & S_{12} \\ S_{12} & -S_{11} \end{pmatrix}$$

in the direction of the principal axes are obtained. For an incompressible fluid in two dimensions this tensor reads in diagonal form

$$\mathbf{S}' = \begin{pmatrix} S_{max} & 0 \\ 0 & S_{min} \end{pmatrix}$$

with $S_{max} = \sqrt{S_{11}^2 + S_{12}^2}$ and $S_{min} = -\sqrt{S_{11}^2 + S_{12}^2}$. This implies that a fluid element is elongated along one of the principal axes while it is compressed in direction of the second one by the same rate.

According to Joseph [16] the elongational stress S_{max} can cause cavitation if the following criterion is fullfilled:

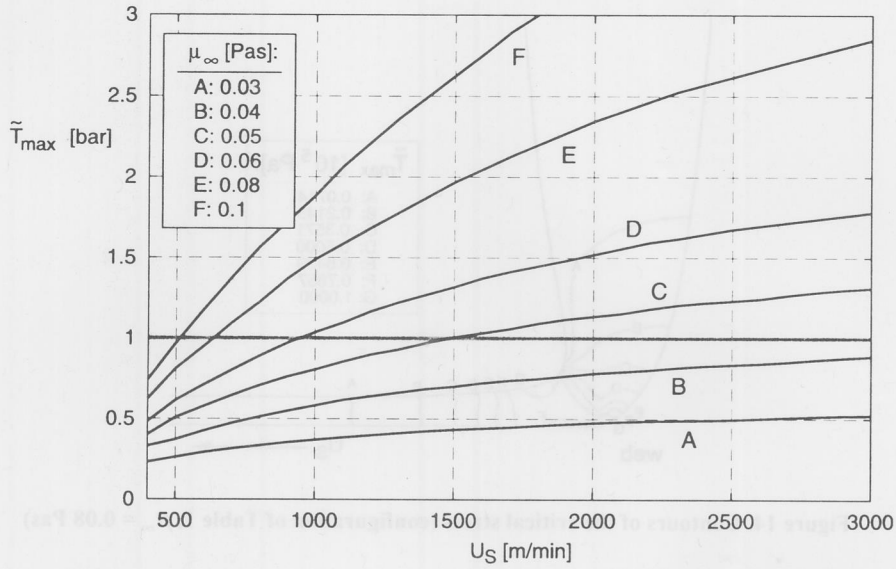

Figure 15. Maximum value of critical stress along free surface in dependence on web speed for different viscosities μ_∞

$$\mathbf{T}_{\max} + p_c = \mathbf{S}_{\max} - (p - p_c) > 0 .$$

Separating the influence of the constant atmospheric pressure p_a which sets the pressure level in free surface flows by introducing $\tilde{\mathbf{T}}_{\max} = \mathbf{T}_{\max} + p_a$ and neglecting the vapor pressure p_c over p_a for usual operating conditions at ambient temperature, the cavitation criterion reads

$$\tilde{\mathbf{T}}_{\max} > p_a$$

In [25, 26] the maximum stress $\tilde{\mathbf{T}}_{\max}$ has been computed in the impingement region of the curtain. Figure 14 shows contours of $\tilde{\mathbf{T}}_{\max}$ for a configuration according to Table 1, but with $\mu_\infty = 0.08$ Pas. It turns out that the critical value of $\tilde{\mathbf{T}}_{\max}$ of about 1 bar is exceeded in a region close to the contact line of the curtain and in a region near the front free surface. The results imply that in curtain coating flow shear stress may cause rupture of the liquid film due to cavitation, even though the classical criterion for cavitation, *i. e.* $p < p_c$ is far from being fullfilled. Cavitation therefore sets an upper limit for the operation of curtain coating, since $\tilde{\mathbf{T}}_{\max}$ increases with increasing web speed (Fig. 15). Also the limiting viscosity, μ_∞, has a strong influence on the onset of cavitation (Fig. 15): While for a

viscosity $\mu_\infty \leq 0.04$ Pas web speeds up to 3000 m/min can be achieved, the critical web speed for the onset of cavitation decreases drastically with increasing μ_∞, dropping from $U_c = 1500$ m/min for $\mu_\infty = 0.05$ Pas down to 500 m/min for $\mu_\infty = 0.1$ Pas. With other words: reducing the limit viscosity by a factor of 2 allows for a about 3 times higher production speed. Another small step of 25% down from $\mu_\infty = 0.05$ Pas to $\mu_\infty = 0.04$ Pas even doubles the critical web speed once more, enhancing the range of operation, *i. e.* the width of the coating window, dramatically.

DRYING

In a thermal drying process heat is supplied to the liquid film to evaporate the solvent and to immobilize the coating layer. Conventional air-impingement and floatation dryers exploit the high heat and mass transfer rates of air jets impinging with high velocity on the coated substrate. Large flow rates of the drying air have to be heated up and eventually low concentrations of the solvent vapor have to be removed from the exhaust air in such dryers. The drying process therefore consumes a considerable amount of energy and requires an exhaust air treatment to avoid environmental hazards when using organic solvents. Modeling a drying process requires a suitable mathematical description of the heat and mass transport within the liquid film and a quantitative characterization of the ability of the drying air to supply heat to the film and to carry away the solvent vapor from the film surface. This essentially implies a coupled solution of the flow, heat and mass transport in the liquid film and in the drying gas [1, 27]. In order to arrive at a simpler low-dimensional model for process engineering dryer design, the gas phase and the liquid film are decoupled by introducing averaged heat and mass transfer coefficients in the boundary conditions for the film surface. This approach was taken up in [6, 7] in a numerical working tool for modeling drying of a binary mixture in a modular air impingement dryer. Besides the concentration profile and the temperature in the film along the dryer, mass and energy balances over the modules give an insight into energy consumption, air flow rates and solvent concentrations in the exhaust air. In this way parameter studies for optimization of the performance of impingement dryers can be efficiently carried out.

The concept of direct condensation drying to be described here in more detail, abandons, however, forced convection as means of enhancing heat and mass transport, aiming at a significant reduction of energy consumption linked with the possibility of the recovery of the liquid solvent. In a drying chamber, as shown in Fig. 1(c), the coated web is heated to evaporate the solvent. A moving cooled belt at which the solvent may condense is mounted at close distance to the heated film surface. The condensed solvent is then removed from the drying chamber for solvent recovery. While this drying concept has long been known in principle (Kores: UK-Pat. 1 401 041, 1975; Valmet-Tampella Inc.: CONDEBELT), it has not yet reached broad application. Lacking publicly available information on the drying performance of such a dryer (see, however, [15]), a thorough investigation of the transport processes in the drying chamber has been undertaken recently [1].

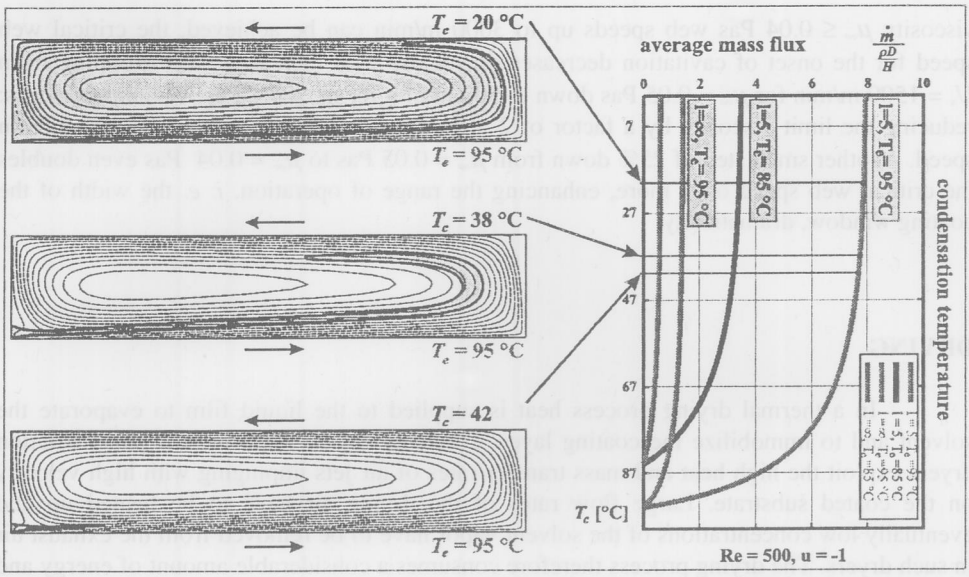

Figure 16. Nucleation in the drying chamber, influence of condensation temperature on evaporation rate, $\mathrm{Re} = U_e H / \nu$, $u = U_e / U_c$, $l = L / H$

In order to get a deeper understanding of the transport mechanisms in the chamber and to obtain a parametrization of the heat and mass transfer coefficients in a drying chamber with heated and cooled moving walls, the flow, heat and mass transport in the gaseous phase of the dryer was computed numerically. The results reveal parameter ranges which achieve potentially high drying rates. A linear stability analysis of the numerical results rules out parameter ranges which are likely to cause unstable operation with the consequence of generating drying defects on the coated film [1]. Near the cooled surface the solvent vapor becomes supersaturated so that the operation range of the dryer is additionally limited by fog formation in the chamber which can damage the film surface. If the drying chamber is encapsulated, particles that serve as nucleation seeds will soon rain off and disappear. Like in a diffusion cloud chamber high supersaturation can then occur, leading to homogeneous nucleation. Using the nucleation criterion of Becker and Döring and Zeldowitsch the fraction of the chamber volume in which fog formation due to homogeneous nucleation will take place has been estimated in [1]. Fig. 16 shows a result of the numerical computations for a water vapor/air mixture at fixed speeds of the web and the cooled belt taken from [1]. The streamlines (dotted lines in Fig. 16) show that the flow of the gas mixture is driven by the motion of the web and the belt, forming a recirculation vortex in the chamber that is slightly distorted by the evaporation mass flux from the heated web to the cooled belt. The area where nucleation occurs (shaded area in Fig. 16) decreases when the condensation temperature T_c is increased and it disappears for condensation temperatures above 42 °C. The shape of that region is determined by convective and

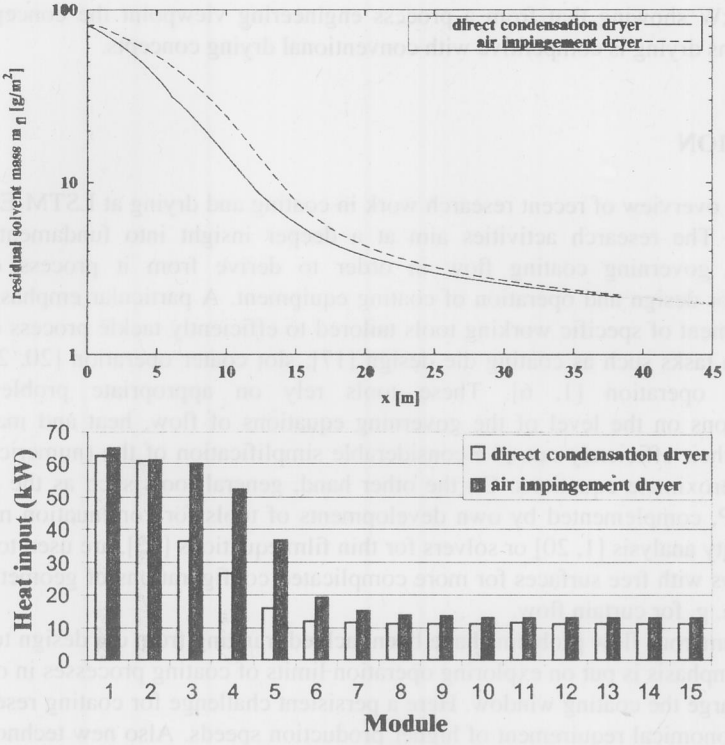

Figure 17. Residual solvent mass in a PVA (20 g/m²)/water (80 g/m²) film (upper), required heat input for the dryer modules (lower)

diffusive transport of the solvent vapor. Even though an increase in condensation temperature decreases the difference in saturation concentration between the cooled belt and the heated film, Fig. 16 (right) shows that the temperature increase necessary to avoid fog formation implies only a very slight decrease of the average evaporation mass flux, so that this operation constraint practically does not influence the drying performance. From the numerical computation of the transport processes in the gaseous phase a parametrization of the heat and mass transfer coefficients was obtained [1] that could be implemented into the working tool for dryer design of [6].

Figure 17 shows a comparative study of the drying performance of a direct condensation dryer and a floatation dryer, each consisting of 15 modules. In both dryers a PVA/water-mixture was dried until a residual solvent content of 2 g/m² was reached. The profile of the residual solvent content along the dryer shows for both dryers a similar behaviour, the condensation dryer shows a slightly higher drying rate in the first modules, however. A comparison of the heat required for drying in each module shows that in the first 6 modules the condensation dryer requires considerably less energy. The total heat required for drying amounts to 314 kW for the condensation dryer while the floatation dryer

needs 417 kW showing that from a process engineering viewpoint the concept of direct condensations drying is competitive with conventional drying concepts.

CONCLUSION

An overview of recent research work in coating and drying at LSTM-Erlangen has been given. The research activities aim at a deeper insight into fundamental physical mechanisms governing coating flow in order to derive from it process engineering guidelines for design and operation of coating equipment. A particular emphasis is put on the development of specific working tools tailored to efficiently tackle process engineering optimization tasks such as coating die design [17], slot coater operation [20, 27] or dryer design and operation [1, 6]. These tools rely on appropriate problem specific approximations on the level of the governing equations of flow, heat and mass transfer. They draw their efficiency out of a considerable simplification of the (numerical) solution of these approximate equations. On the other hand, general tools such as the commercial code FIDAP, complemented by own developments of tools for continuation methods [1], linear stability analysis [1, 20] or solvers for thin film equations [25], are used to investigate coating flows with free surfaces for more complicated configurations of geometry and fluid properties, e. g. for curtain flow.

Numerous flow problems have been tackled, ranging from die design to drying. A particular emphasis is put on exploring operation limits of coating processes in order to find ways to enlarge the coating window. Here a persistent challenge for coating research comes from the economical requirement of higher production speeds. Also new technologies as *e. g.* digital printing require an improved quality of papers with reduced area weight and less pigment consumption driving the search for new and improved coating methods.

REFERENCES

[1] Alleborn, N.: *Untersuchung der Strömung und des Wärme- und Stofftransports in einer Trocknerkammer*, Dissertation, Universität Erlangen-Nürnberg, 2001,

[2] Alleborn, N., Raszillier, H., Durst, F.: Lid-driven cavity with heat and mass transport, *Int. J. Heat Mass Transf.* 42 (1999), pp. 833-853,

[3] Alleborn, N., Raszillier, H., Durst, F.: Linear stability of non-Newtonian annular liquid sheets, *Acta Mechanica* 137 (1999), pp. 33-42,

[4] Alleborn, N., Raszillier, H., Durst, F.: Propagation of disturbances in thin viscous liquid sheets, In: *10th International Coating Science and Technology Symposium – Final Program and Extended Abstracts*, ICST – International Society of Coating Science and Technology, Scottsdale, Arizona, September 25-27, 2000, pp. 40-43,

[5] Archer, L.A., Ternet, D., Larson, R.G.: Fracture phenomena in shearing flow of viscous liquids, *Rheol. Acta* 36 (1997), pp. 579-584,

[6] Aust, R.: *Verfahrenstechnische Aspekte der Trocknung beschichteter Materialbahnen*, Dissertation, Universität Erlangen-Nürnberg, 1996,

[7] Aust, R., Durst, F., Raszillier, H.: Modeling a multiple-zone air impingement dryer, *Chem. Eng. Proc.* 36 (1997), pp. 469-487,

[8] Cohen, E.D., Gutoff, E.B. (eds.): *Modern coating and drying technology*, VCH Publ., New York, 1992,

[9] Durst, F., Raszillier, H. (eds): *Advances in Coating and Drying of Thin Films: 3rd European Coating Symposium 1999*, Shaker-Verlag, Aachen, 1999,

[10] Durst, F., Wagner, H.G: Slot coating, In: Kistler, S.F., Schweizer, P.M. (eds.): *Liquid film coating*, Chapman & Hall, London, 1997,

[11] Durst, F., Sünderhauf, G., Troller, U., Schweizer P.M.: Flow in a two-cavity die, comparative study between analytical model, finite element analysis and experiment, In: Bourgin, P. (ed.): *EUROMECH 367 – Fluid Mechanics of Coating Processes*, Proceedings of the Second European Coating Symposium (ECS'97), University Louis Pasteur, Strasbourg, July 22-25, 1997, (1996), pp. 382-391,

[12] Durst, F., Sünderhauf, G., Raszillier, H.: Papierbeschichtung mit einer Rakel , Teil I: Strömungsphysikalische Modellierung, *Coating* 9/96 (1996), pp. 326-331,

[13] Durst, F., Sünderhauf, G., Raszillier, H.: Papierbeschichtung mit einer Rakel , Teil II: Ergebnisse numerischer Simulationen, *Coating* 11/96 (1996), pp. 424-428,

[14] Gumbrecht, M., Sünderhauf, G., Raszillier, H., Durst, F.: Die Rollrakel als Dosierelement in der Beschichtungstechnik von Flüssigkeitsfilmen, *Wochenblatt für Papierfabrikation*. 10 (1999), pp. 699-704,

[15] Huelsman, G.L., Kolb, W.B.: Coated substrate drying system, World Intellectual Property Organization, Int. Publication No. WO 97/11328. 1997,

[16] Joseph, D.D.: Cavitation and the state of stress in a flowing liquid, *J. Fluid Mech.* 366 (1998), pp. 367-378,

[17] Lange, U.: *Strömungsmechanische Optimierung von Komponenten einer Vorhangbeschichtungsanlage*, Dissertation, Universität Erlangen-Nürnberg, 1995,

[18] Kistler, S.F.: *The fluid mechanics of curtain coating and related viscous free surface flows with contact lines*, PhD-thesis, University of Minnesota, 1984,

[19] Kistler, S.F., Schweizer, P.M. (eds.): *Liquid film coating*, Chapman & Hall, London, 1997,

[20] Müller, Ch.: *Strömungsanalyse der Vorhangbeschichtung*, Dissertation, Universität Erlangen-Nürnberg, 2000,

[21] Raszillier, H., Alleborn, N., Durst, F.: Mode mixing in Coriolis Mass Flowmetering, *Arch. Appl. Mech.* 63 (1994), pp. 219-227,

[22] Secor, R.B.: Analysis and design of internal coating die cavities, In: Kistler, S.F., Schweizer, P.M. (eds.): *Liquid film coating*, Chapman & Hall, London, 1997,

[23] Stadler, D.: *Strömungsmechanik des Papierstreichens*, Dissertation, Universität Erlangen-Nürnberg, 1996,

[24] Streator, J.L., Gerhardstein, J.P., McCollum, C.B.: The low-pressure rheology of ultra-thin lubricant films and its influence on sliding contact, *J. Tribology* 116 (1986), pp. 119-126,

[25] Sünderhauf, G.: *Strömungsuntersuchung des Vorhangstreichens von Papier*, Dissertation, Universität Erlangen-Nürnberg, 2001,

[26] Sünderhauf, G., Raszillier, H., Durst, F.: Curtain Coating of Paper at High Speed – Fluid Dynamical Limitations, submitted to *TAPPI-Journal*.

[27] Wagner, H.G.: *Die Schlitzfließerbeschichtung und Laminartrocknung als Grundverfahren optimierter Beschichtungsanlagen.* Dissertation, Universität Erlangen-Nürnberg, 1996.

Author's address:

Dr.-Ing. Norbert Alleborn
Lehrstuhl für Strömungsmechanik,
Universität Erlangen-Nürnberg
Cauerstr. 4
D-91058 Erlangen
Germany

Paper submitted: November 30, 2001
Paper revised: February 26, 2002
Paper accepted: March 18, 2002